ISOTOPIC AND MICROSTRUCTURAL ANALYSES OF OPAQUE MINERAL ASSEMBLAGES AND THEIR ALTERATION PRODUCTS HOSTED IN A REFRACTORY INCLUSION. P. Mane[1,2,3] , T. J. Zega[3], A. N. Nguyen[2,4], J. I. Simon[2], , [1]Lunar and Planetary Institute, USRA, 3600 Bay Area Boulevard, Houston, TX 77058 USA (pmane@lpi.usra.edu), [2]EISD/Astromaterials Research and Exploration Sciences, NASA Johnson Space Center, 2101, NASA Parkway, Houston, TX 77058 USA, [3]Lunar and Planetary Laboratory, University of Arizona, Tucson, AZ, 85721, [4]Jacobs, Houston, TX, 77058, USA.

Introduction: Calcium-aluminum-rich inclusions (CAIs) hosted in primitive meteorites are the oldest solids formed in the Solar System [e.g., 1]. Some CAIs contain metal nuggets that are complex assemblages of Fe-Ni alloys, along with rare ultra-refractory metals such as platinum group elements (PGEs), and their alteration products such as magnetite, sulfides, and phosphates [e.g., 2,3,4]. Three possible mechanisms proposed to explain the origin of these metal nuggets include condensation in circumstellar settings, condensation in the solar nebula within the CAI-forming region, or crystallization from immiscible metal-silicate melt [2,3]. However, secondary alteration processes may have also affected some of these assemblages [e.g., 4,5]. Additionally, similar metal assemblages observed in chondrules and chondritic matrix indicate that all of these metal nuggets could share common high-temperature origins [6]. These metal assemblages record early Solar System conditions that are reflected in their distinctive chemical composition, mineralogy and microstructures. Here we report a detailed mineralogical, microstructural and oxygen isotopic study of one such metal assemblage hosted in a CAI to understand the physical and chemical settings in which it formed.

Sample Description: The metal assemblages studied here occur within a compact type-A inclusion ("Hedgehog") from the NWA 5028 CR2 chondrite. Hedgehog is primarily dominated by melilite, spinel, and perovskite. The Wark-Lovering rim [7] around Hedgehog contains an innermost layer of spinel, hibonite, and perovskite, followed by a middle layer of melilite, and an outermost layer of diopside. Silicate minerals in Hedgehog define an Al-Mg isochron with an initial $^{26}Al/^{27}Al$ ratio of $(6.0 \pm 1.1) \times 10^{-5}$ that is indistinguishable from the canonical value [8].

Methods: We investigated the metal assemblages using a CAMECA SX-100 electron microprobe at the Lunar and Planetary Laboratory (LPL), University of Arizona to obtain backscattered electron (BSE) images, wavelength dispersive x-ray spectrometry (WDS) spot analyses, and element maps of selected regions. We further investigated these regions using the Thermo Fisher (formerly FEI) Helios NanoLAB 660 G^3 focused-ion beam scanning-electron microscope (FIB-SEM), equipped with an EDAX energy dispersive x-ray spectrometer (EDS) and electron backscatter diffraction (EBSD) detector, located at LPL. An assemblage consisting of metal and perovskite, surrounded by spinel and melilite, was sectioned and extracted using the EasyLift micromanipulator on the Helios and thinned to electron transparency using previously described methods [9]. The FIB section was ion polished down to 5 keV, to remove the amorphous damage layer created by higher-voltage milling, and subsequently analyzed using the 200 kev Hitachi HF50000 transmission electron microscope (TEM) at LPL. The HF5000 is aberration corrected in scanning TEM (STEM) mode and is equipped with a cold-field emission gun, STEM-based bright-field (BF) and dark-field (DF) detectors, as well as an Oxford Instruments X-max large solid angle (2 sr) energy-dispersive X-ray spectrometer (EDS).

Oxygen isotopic imaging of the oxide, phosphate, and silicate phases in Hedgehog was performed using the Cameca NanoSIMS 50L ion microprobe at NASA Johnson Space Center (JSC). We followed the analytical protocol described in [10]. The O-isotopic maps of the metal assemblages were acquired by rastering a ~1.5 pA primary Cs^+ beam at 16 keV over an area of 20 × 20 μm^2 for 80 image planes (period of ~7 hours). Negative secondary ions of $^{16}O^-$, $^{17}O^-$, $^{18}O^-$, and $^{28}Si^-$ were simultaneously acquired using electron multiplier detectors at a mass resolving power of >10,000, sufficient to resolve the $^{16}OH^-$ interference from the $^{17}O^-$ peak. An electron flood gun was used to mitigate sample charging during the analyses. We used San Carlos olivine as an isotopic standard to correct for the instrumental mass fractionation. The O-isotopic ratios were corrected for the quasi simultaneous arrival (QSA) effect and the detector dead time [9].

Results and Discussion: The metal assemblages are composed of an Fe-Ni-Co alloy (Fig. 1). The Fe content varies from 45 to 90 wt%, whereas the Ni content varies from 6 to 48 wt%. Cobalt occurs as a minor element (up to 3 wt%). No refractory PGEs were detected in the metal phases. EBSD analysis (Fig. 2) shows that the individual metal grains are euhedral, suggesting crystallization from a melt. The metal nuggets show subsolidus exsolution into kamacite and taenite, where the high-Ni and low-Ni phases occur as lamellae arranged in preferred orientation. Most metal grains contain Fe-oxide inclusions, with abundant V (up to 17 wt

%) and Cr (up to 8 wt%). The metal assemblages show rims of Fe-oxide and phosphates around them.

The oxygen isotopic analysis (Fig. 3) of several oxide grains inside the metal and oxide and phosphate rim surrounding the metal reveals an ^{16}O-poor isotopic composition, falling on the terrestrial fractionation line. The host melilite shows $\Delta^{17}O = -8 \pm 2.9‰$ that plots below the TMF line, but is still relatively ^{16}O-poor for a nebular product. The ^{16}O-poor isotopic composition of these oxide phases suggests that they formed as a result of alteration of the metal assemblages in a parent-body setting (see below).

A FIB section sampling spinel, metal, perovskite, and part of the melilite was created to analyze the metal-silicate phase boundary in more detail. The metal grain contains a subhedral morphology and its upper interface with spinel contains a triple junction. DF imaging of the metal grain reveals non-uniform atomic-number (Z) contrast, which EDS mapping shows is due to Ni-poor and Ni-rich domains. SAED patterns of the Ni-rich domain are consistent with taenite, whereas those so far acquired from the Ni-poor domain index to Fe metal. The interface between the perovskite and the metal contains several layers of material with varied Z-contrast. EDS mapping shows that these layers consist of (a) an Fe-Mg-O phase; (b) a Ca-P-O phase; and (c) an Fe-Mg-Ti-O phase.

The textures and composition of compact type-A CAIs indicate they were thermally processed, i.e., either partially heated or some may have crystallized from a melt [11]. The metal nuggets in Hedgehog show exsolution lamellae suggesting that the metal either formed as a crystallization product possibly during this thermal processing or was reprocessed during the thermal event, within the first ~70,000 years after CAI formation [8]. The oxygen isotopic composition of the Fe-oxides suggests that alteration subsequently occurred in a parent body setting. The Fe-oxide inclusions in the metal as well as Fe-oxide, sulfide, and phosphate layers around the metal suggest a complex history with possible multiple episodes of aqueous alteration on the CR2 meteorite parent body.

References: [1] Connelly J. N. et al. (2012) *Science* 338:651-655. [2] El Goresy A. et al. (1997) *Meteoritics* 12:215-216. [3] Wark D. A. and Lovering J. F. (1976) *7th Lunar and Planetary Science* 912-914. [4] Bischoff, A., & Palme, H. (1987) *Geochimica et Cosmochimica Acta*, 51(10): 2733-2748. [5] Armstrong, John T. et al. (1987) *Geochimica et Cosmochimica Acta* 51:3155-3173. [6] Daly L. et al. (2017) *Geochimica et Cosmochimica Acta*. [7] Wark D. A. and Lovering J. F. 1977. *Proc Lunar Planet. Sci. Conf. 8th:* pp. 95-112. [8] Mane P. et al. (2016) *Meteoritics & Planetary Science* 51S1:300. [9] Zega T. J. et al. (2007) *Meteoritics & Planet. Sci.,* 42:1373-1386. [10] Ito M. & Messenger S. (2008) *Appl. Surf. Sci.* 255:1446-1450. [11] Simon S.B., Davis A.M., and Grossman L. (1999) GCA 63:1233-1248.

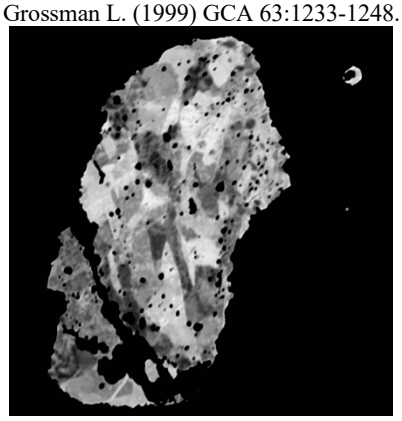

Figure 1. Low brightness BSE image of Metal Grain: The grey scale variation is due to Ni-Fe-Co variation. The Fe-V-Cr oxides in the metal can be seen as black inclusions.

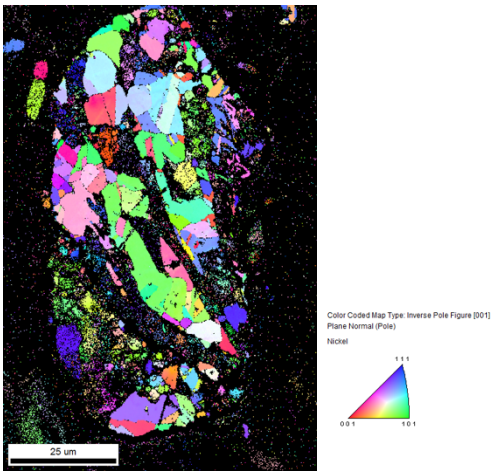

Figure 2. Inverse pole figure maps of a metal assemblage from Hedgehog showing high-Ni and low-Ni phases occur as lamellae arranged in preferred orientation.

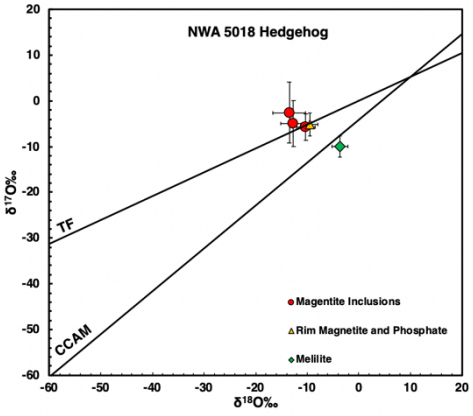

Figure 3 Oxygen isotopic composition of Fe-V-Cr oxide inclusions as well as oxide and phosphate layers in the metal assemblage. Errors plotted here are 1σ.